ingegneria sismica
International Journal of Earthquake Engineering
Anno XLIII - Num. 3 - 2026

Polishing Process Optimization of Aluminosilicate Glass Based on Response Surface Method

Peng Zhao[1], *Da Bian*[1,2,*], *Shanhua Qian*[1,2] *and Zifeng Ni*[1,2]

[1] School of Mechanical Engineering, Jiangnan University, Wuxi, 214122, Jiangsu, China
[2] Jiangsu Key Laboratory of Advanced Food Manufacturing Equipment & Technology, Jinagnan University, Wuxi, 214122, Jinagsu, China

SUMMARY: *In order to optimize the polishing rate and surface quality of chemical mechanical polishing of aluminosilicate glass by adjusting the process parameters, the response surface method was used to determine the optimal process of polishing pressure, slurry flow rate and polishing plate speed. The results show that the influence of polishing pressure, polishing disc speed and polishing liquid flow rate on the material removal rate decreases in turn. The influence of polishing pressure, slurry flow rate and polishing disc speed on the roughness decreases in turn. The optimum process parameters are polishing pressure of 3.6 kg, polishing liquid flow of 71 mL / min and polishing disc speed of 110 r / min. The experimental results show that the measured material removal rate under this condition is 196.306 nm / min, and the surface roughness of the polished glass is as low as 1.260 nm, which realizes the joint optimization of polishing rate and surface quality.*

KEYWORDS: *chemical mechanical polishing; process parameters; response surface method; aluminosilicate glass*

1 Foreword

Among many special glass systems, aluminosilicate glass stands out because of its unique advantages. Aluminosilicate glass has the core advantages of high strength, high heat resistance, high chemical stability, low expansion and high light transmittance. It is widely used in electronics, automobile, optics, aviation, industry, photovoltaic solar energy and other fields[1-3]. Based on the current wide application, higher requirements are put forward for the surface quality of aluminosilicate glass. Aluminosilicate glass is a typical brittle and hard material, which has the disadvantages of high hardness, high brittleness and poor machinability. How to improve the processing efficiency and surface quality of aluminosilicate has become one of the most important factors restricting its wide application. Chemical Mechanical Polishing (CMP) can be achieved via precise control of slurry composition and process parameters, to achieve ultra-precision machining of workpiece surfaces[4, 5], to yield a globally planarized surface[6]. CMP process parameters are among the key factors governing polishing performance[7]. Therefore, tight control of process parameters is required to achieve high material removal rate and low surface roughness. Parthiban et al.[8] investigated the effect of slurry flow rate on GaN CMP performance using $KMnO_4/Al_2O_3$-based slurry, confirming that moderately increasing the flow rate enhances material removal rate and optimizes surface quality, whereas excessive flow

*jiangnan6230805148@163.com
https://doi.org/10.65102/is20261247
Published: 10 June, 2026

rate degrades polishing performance; Mudhivarthi et al.[9] revealed the modulation effect of slurry flow rate on interfacial heat dissipation, reaction equilibrium and surface corrosion; Forsberg et al.[10] experimentally investigated the effects of process parameters on the material removal rate (MRR) of Si(100) during CMP, confirming that the Si(100) MRR increases sublinearly with polishing pressure, platen rotational speed and slurry silica concentration; Huang et al.[11] systematically investigated the effects of parameters such as platen rotational speed on the polishing performance of ceramic blocks. They demonstrated that increasing rotational speed improves material removal rate and optimizes surface roughness. Diamond particle size is the most significant factor affecting removal rate and surface quality, and three main failure mechanisms exist in ceramic polishing: cracking, deep pitting, and fracture.

2 Materials and Methods

2.1 Experimental Materials and Equipment

Chemical mechanical polishing (CMP) tests were conducted on aluminosilicate glass wafers with a radius of 20 mm, using a UNIPOL-1200S precision polishing machine manufactured by Shenyang Kejing Equipment Co., Ltd. The matching polyurethane polishing pad was supplied by Beijing Mingchen Zhonghuan Technology Co., Ltd. All experiments were performed at a constant temperature of 25 °C, with a polishing time of 20 min. Before and after polishing, all wafers were ultrasonically cleaned for 5 min sequentially in 95% anhydrous ethanol (Sinopharm Chemical Reagent Co., Ltd.) and deionized water to completely remove surface impurities and residual polishing media. The cerium-based polishing slurry employed was self-developed by our research group. Mass changes of the wafers were measured with an XS205DU high-precision balance (Mettler Toledo, Switzerland). Triplicate parallel weighings were carried out for each sample to guarantee accuracy and reliability, and the arithmetic mean was adopted as the final result. The material removal rate (MRR) of aluminosilicate glass was quantitatively calculated by the weight loss method based on mass variation data. Surface roughness of the polished wafers was characterized by an MFP-D white light interferometer (RTEC, USA) with a scanning area of 50 μm × 50 μm. Three random positions on each wafer were selected for triplicate parallel tests, and the arithmetic mean of all measurements was taken as the final surface roughness value.

2.2 Experimental Procedure

(1) Chemical mechanical polishing experiments

In this chapter, material removal rate (MRR) and surface roughness (Ra) were chosen as the core performance evaluation indexes. The process parameter optimization for chemical mechanical polishing of aluminosilicate glass was systematically carried out through a three-stage progressive experimental scheme. In the first stage, single-factor variable-control experiments were performed to explore the effects of three key parameters (polishing pressure, platen rotational speed and slurry flow rate) on the polishing performance of optical glass, so as to determine their effective value ranges. The initial parameter ranges were determined by referring to relevant studies and our preliminary experimental data, with the detailed design listed in Table 1. In the second stage, based on the Box-Behnken response surface methodology, a quadratic multiple regression model was established between key process parameters and core polishing performance indexes. Analysis of variance (ANOVA) was used to verify the significance and fitting reliability of the regression model. In the third stage, global optimization was implemented via an optimization algorithm to achieve the optimal trade-off between maximized MRR and minimized Ra. The optimal process parameter combination suitable for

CMP of aluminosilicate glass with self-made composite abrasives in our laboratory was finally obtained.

Table 1: Single-factor experimental parameters

experimental group	Polishing pressure/kg	Polishing liquid flow rate/(mL/min)	Polishing disc speed/(r/min)
A	1.5, 2.5, 3.5, 4.5, 5.5	50	50
B	2.5	30, 50, 70, 90, 110	50
C	2.5	70	30, 50, 70, 90, 110

3 Results and Discussion

3.1 Effect of Polishing Pressure on CMP Performance of Aluminosilicate Glass

Fig.1 shows the evolution of MRR and Ra for aluminosilicate glass with polishing pressure during chemical mechanical polishing. The material removal rate shows a nonlinear trend rather than a linear positive correlation with polishing pressure: it rises sharply first and then decreases obviously. As the polishing pressure increases from 1.5 kg to 4.5 kg, MRR increases continuously by 218.5%; when the pressure further rises to 5.5 kg, MRR decreases by 18.0% instead. Under low pressure, insufficient effective contact between abrasives and the glass surface impedes the activation of the piezocatalytic effect of piezoelectric abrasives, limiting the generation of reactive oxygen species and slowing the surface hydroxylation of glass. Meanwhile, weak mechanical grinding fails to fully break the interfacial Ce-O-Si bonds, leading to a low MRR[12, 13]. With increasing pressure, the effective contact area and the number of effective grinding abrasives increase significantly, and the synergistic effects of piezoelectric response, chemical etching and mechanical grinding are enhanced simultaneously, driving a rapid rise in MRR. Beyond 4.5 kg, excessive load causes the collapse of the mesoporous structure of abrasives and the loss of active sites, together with abrasive agglomeration that reduces grinding efficiency, eventually resulting in a decline in material removal rate.

The surface roughness of the aluminosilicate glass substrate first decreases significantly and then rises continuously with increasing polishing pressure. The smoothest surface within the experimental range is obtained at 3.5 kg. Under low pressure, the effective abrasives are limited and loosely distributed, failing to uniformly remove micro-protrusions on the glass surface, thus resulting in poor polishing uniformity and high surface roughness. As pressure increases, the abrasive packing density rises and the chemo-mechanical synergistic effect is greatly strengthened, making roughness drop continuously. At 3.5 kg, a dynamic equilibrium between chemical modification and mechanical grinding is achieved, giving the minimum roughness. When pressure exceeds the critical value, excessive mechanical loading induces brittle damage on the glass surface[14]. Meanwhile, hard debris from the fractured mesoporous abrasive shell under high pressure causes secondary scratching, which eventually leads to a continuous increase in surface roughness.

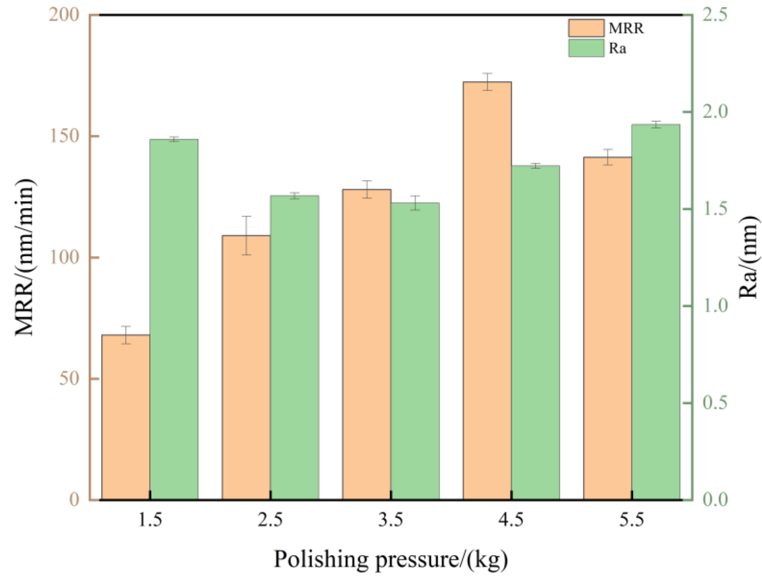

Figure 1: variations of MRR and Ra of glass with polishing pressure

Fig.2 shows the 3D surface morphologies of aluminosilicate glass after CMP under different polishing pressures. The surface quality is optimal at 3.5 kg, and good flatness is obtained at 2.5 and 4.5 kg. The glass exhibits under-polishing at 1.5 kg and obvious processing damage at 5.5 kg. Based on the key performance indicators, the preferred polishing pressure range is 2.5–4.5 kg.

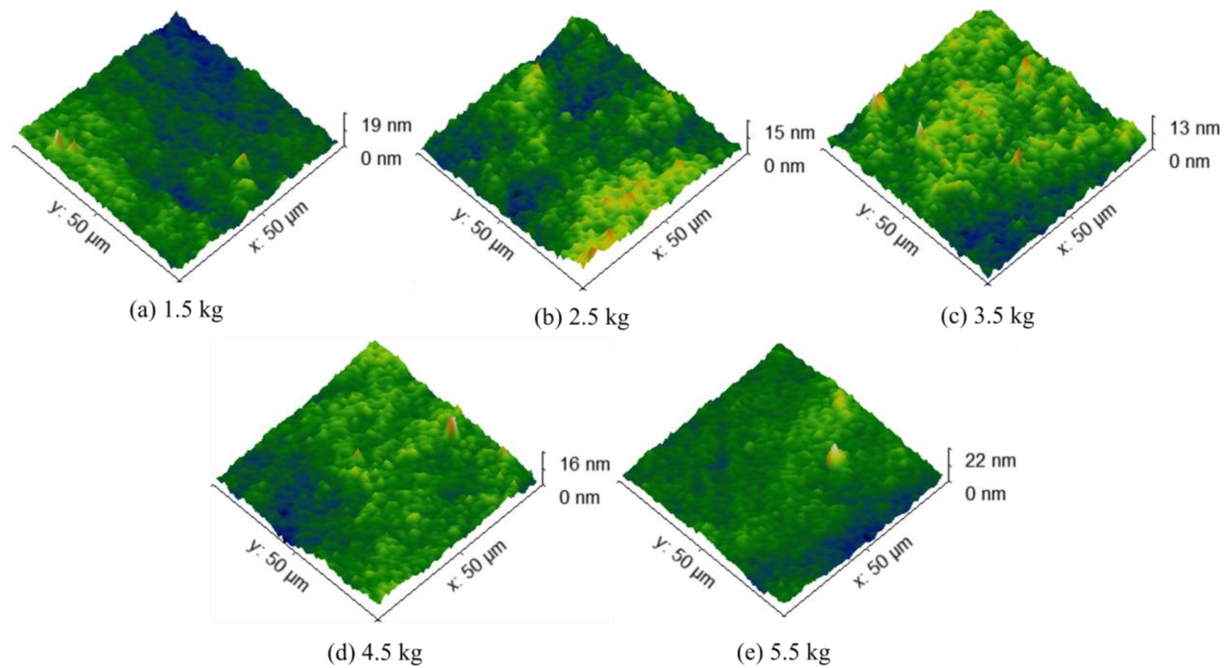

Figure 2: surface morphologies of glass polished under different polishing pressures

3.2 Effect of Polishing Liquid Flow Rate on CMP Performance of Aluminosilicate Glass

Fig.3 presents the evolution of MRR and Ra for aluminosilicate glass with polishing liquid flow rate during CMP.MRR is positively correlated with flow rate, but its growth rate gradually

diminishes with rising flow rate, and the regulatory effect of flow rate is significantly weaker than that of polishing pressure. As the flow rate increases from 30 mL/min to 110 mL/min, the total increment of MRR is 62.1%.At a low flow rate of 30 mL/min, insufficient fresh abrasives are supplied to the polishing interface and reaction byproducts cannot be discharged in time, which restricts the effective contact between abrasives and glass, leading to the lowest MRR. With increasing flow rate, interfacial abrasives are continuously renewed, the chemical effect of active sites is fully exerted, and byproducts are removed promptly[15], driving a steady increase in MRR. Nevertheless, increasing flow rate has marginal limitations: the residence time of abrasives at the interface is shortened so that they are carried away before full functioning. Meanwhile, liquid flow scouring lowers the interfacial temperature and inhibits surface hydrolysis and chemical bond formation, eventually causing the growth rate of MRR to keep narrowing.

The surface roughness of aluminosilicate glass first decreases and then increases with rising slurry supply flow rate, and the smoothest surface in the experimental range is obtained at 70 mL/min. Under low flow rates, insufficient effective abrasives, uneven load distribution and limited debris removal cause brittle damages (e.g., scratching and pitting) on the glass surface due to retained debris, resulting in markedly high surface roughness.As the flow rate reaches 70 mL/min, an optimal balance is achieved among abrasive supply, debris elimination, and interfacial lubrication/cooling, with abrasives evenly dispersed, thus minimizing surface roughness. When exceeding this critical value, a fluid buffer film readily forms at the interface, hindering stable and effective abrasive–glass contact. High-speed flow also disrupts abrasive distribution and polishing stability, eventually leading to a continuous increase in surface roughness.

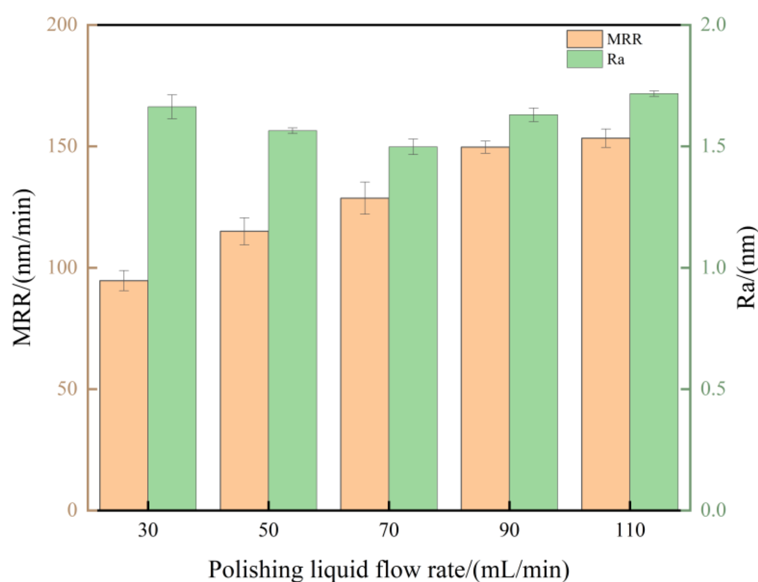

Figure 3: variations of MRR and Ra of glass with polishing liquid flow rate

Fig.4 displays the 3D surface morphologies of aluminosilicate glass after CMP under different slurry flow rates. The surface quality is optimal at 50 and 70 mL/min, while other flow rate groups exhibit varying degrees of processing defects, which is consistent with the variation law of surface roughness. According to the core performance indicators, the preferred slurry flow rate range is 50–90 mL/min.

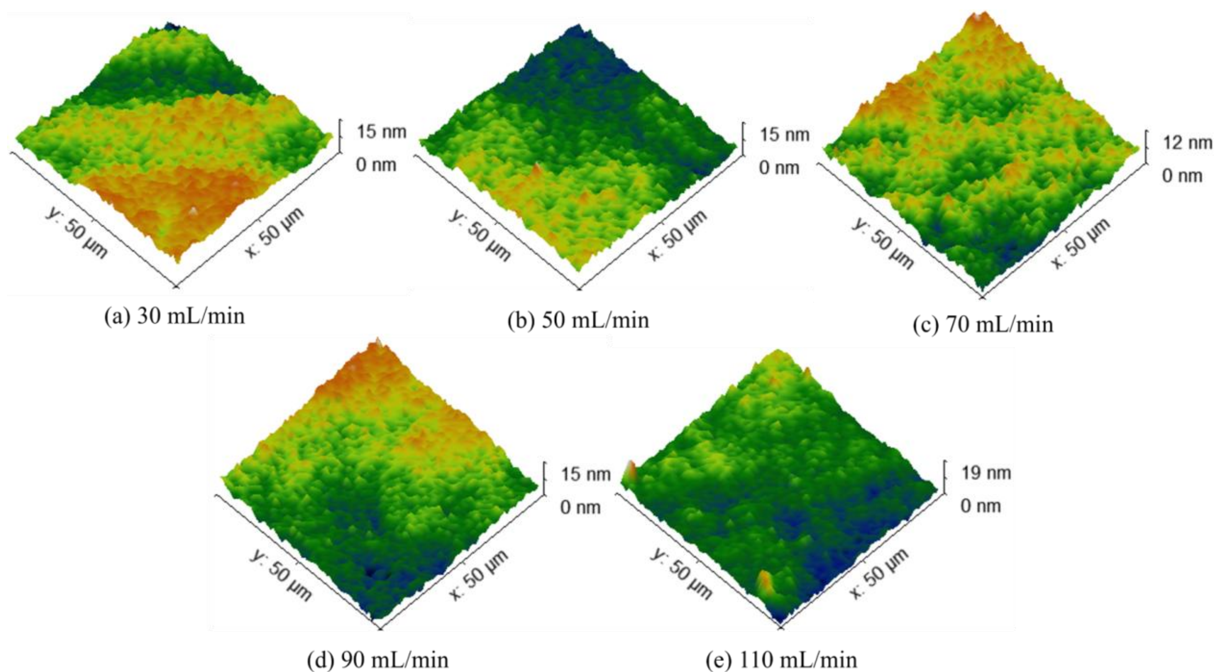

Figure 4: surface morphologies of glass polished under different polishing liquid flow rate

3.3 Effect of Polishing disc Speed on CMP Performance of Aluminosilicate Glass

Fig.5 shows the evolution of MRR and Ra for aluminosilicate glass with polishing disc speed during CMP. The results reveal a strong positive correlation between material removal rate and platen speed, with the removal efficiency being extremely low at 30 r/min. This phenomenon can be mainly ascribed to three reasons. First, the contact frequency between core–shell abrasives and the glass surface is insufficient at low speed, accompanied by weak interfacial mechanical shear stress. Second, insufficient centrifugal force restricts interfacial fluid transport, lowering the supply efficiency of fresh abrasives and the discharge rate of reaction products. Third, the low frequency of alternating stress fails to effectively activate the piezocatalytic effect of barium titanate cores, inhibiting the generation of reactive oxygen species (e.g., hydroxyl radicals) and slowing the hydrolysis of Si-O-Si bonds on the glass surface. Consequently, the material removal rate remains at a low level.

The surface roughness of aluminosilicate glass first decreases and then rises gently with increasing platen speed. It declines continuously from 30 to 90 r/min and reaches the minimum in the test range at 90 r/min. At low speeds, insufficient mechanical grinding cannot uniformly eliminate micro-protrusions on the glass surface. Restricted slurry transport also causes uneven abrasive distribution and unstable polishing, leading to notably high surface roughness. At 90 r/min, the higher frequency of interfacial alternating stress enhances the piezocatalytic effect, realizing uniform hydrolytic softening of the glass surface and minimizing roughness. Above this critical speed, excessive mechanical shear easily induces brittle damage on the glass surface. High-speed rotation also triggers slurry splashing, reducing abrasive uniformity and polishing stability, which eventually results in a continuous rise in surface roughness.

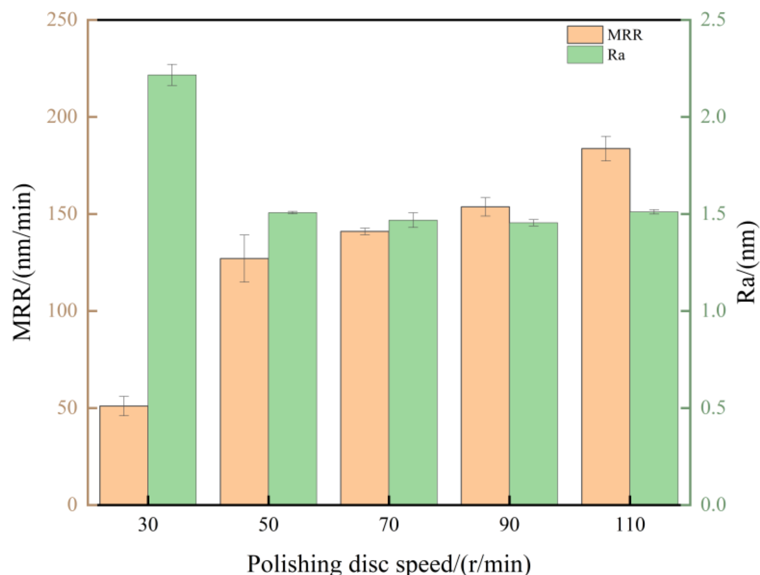

Figure 5: variations of MRR and Ra of glass with polishing disc speed

Fig.6 shows the 3D surface morphologies of aluminosilicate glass after CMP at different platen rotational speeds. The surface flatness is optimal at 70 and 90 r/min, while other speed groups exhibit varying degrees of morphological defects, in accordance with the variation trend of surface roughness. According to the core performance indicators, the preferred rotational speed range is 70–110 r/min.

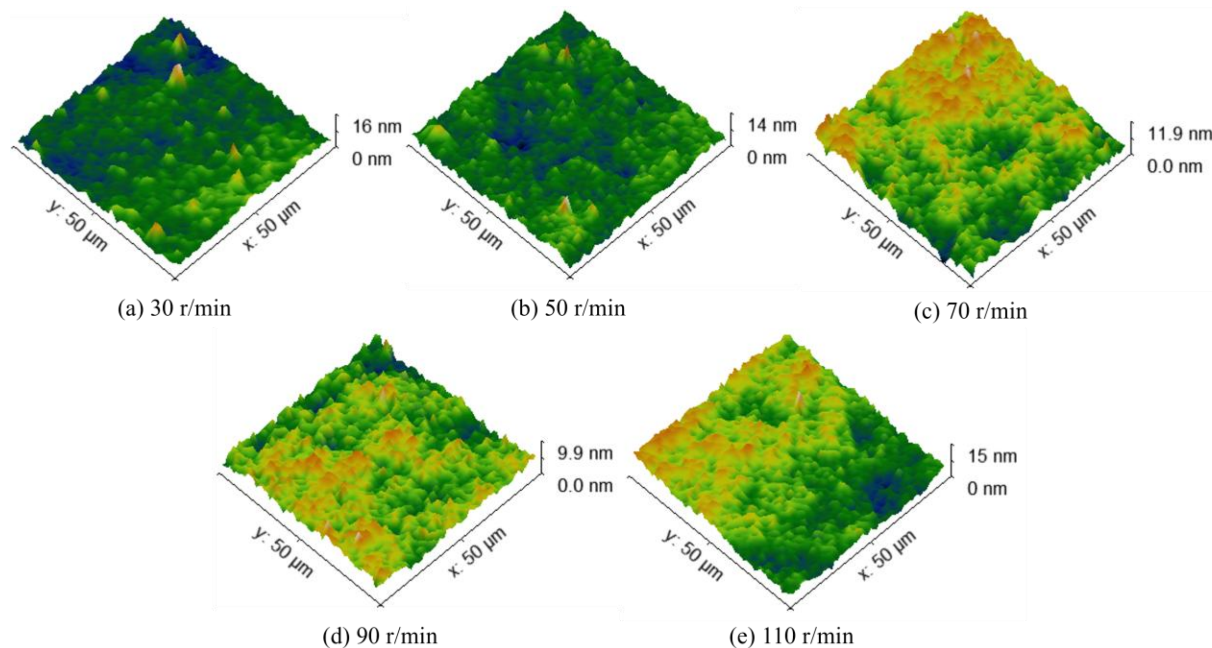

Figure 6: surface morphologies of glass polished under different polishing disc speed

3.4 Response Surface Design and Its Analysis

Based on the influence laws and reasonable ranges of parameters obtained from single-factor experiments, the three-factor, three-level Box-Behnken response surface methodology was adopted for multi-objective process optimization in this chapter, as shown in Table 2.Polishing pressure (X_1), slurry flow rate (X_2) and platen rotational speed (X_3) were taken as independent

variables, while material removal rate (R_1) and surface roughness (R_2) were set as response indices. The experimental scheme was designed using Design-Expert 13.0, with a total of 17 runs including 12 factorial points and 5 central repeated verification points, as listed in Table 3.The levels of each factor were determined according to single-factor tests, enabling accurate quantitative analysis of the main effects and interactions of parameters, thus providing reliable experimental data for establishing high-precision mathematical prediction models.

Table 2: factors and levels of response surface experiments

Factors	Levels		
	-1	0	1
Polishing pressure X_1/kg	2.5	3.5	4.5
Polishing liquid flow rate X_2(mL/min)	50	70	90
Polishing disc speed X_3(r/min)	70	90	110

Table 3: response surface experimental design and results

Run number	X_1	X_2	X_3	R_1	R_2
1	4.5	50	90	172.68	1.59
2	3.5	70	90	144.72	1.29
3	3.5	50	70	117.85	1.42
4	3.5	70	90	146.19	1.31
5	3.5	90	70	152.93	1.49
6	2.5	90	90	146.87	1.54
7	4.5	70	70	174.56	1.55
8	3.5	70	90	143.89	1.28
9	4.5	90	90	211.74	1.67
10	4.5	70	110	221.83	1.57
11	2.5	70	70	112.64	1.44
12	3.5	70	90	145.47	1.30
13	2.5	50	90	111.92	1.47
14	2.5	70	110	155.76	1.44
15	3.5	70	90	144.28	1.32
16	3.5	90	110	195.81	1.49
17	3.5	50	110	160.95	1.42

Based on the established Box-Behnken response surface design, 17 confirmatory CMP experiments on aluminosilicate glass substrates were carried out, and the measured data of material removal rate and surface roughness under various process parameter combinations were collected synchronously. Multivariate nonlinear regression fitting was conducted on the experimental data set via Design-Expert 13.0 software. Second-order polynomial response surface prediction models for material removal rate and surface roughness were finally established, with their mathematical expressions presented in Eqs. (1) and (2), respectively.

$$\begin{aligned} R_1 = {} & 270.38062 - 64.78000 * X_1 - 0.419250 * X_2 - 2.97788 * X_3 \\ & + 0.051375 * X_1 * X_2 + 0.051875 * X_1 * X_3 - 0.000138 * X_2 * X_3 \\ & + 12.60250 * X_1^2 + 0.008225 * X_2^2 + 0.021713 * X_3^2 \end{aligned} \tag{1}$$

$$R_2 = 5.21969 - 1.06375 * X_1 - 0.037562 * X_2 - 0.020438 * X_3 \\ +0.000125 * X_1 * X_2 + 0.000250 * X_1 * X_3 + 0.000000 * X_2 * X_3 \\ +0.156250 * X_1^2 + 0.000278 * X_2^2 - 0.000109 * X_3^2 \quad (2)$$

Analysis of variance (ANOVA) was performed to verify the significance of the two response surface prediction models, as shown in Tables 4 and 5.Both models have P-values < 0.0001, indicating extremely high statistical significance. The lack-of-fit terms have P-values > 0.05 and are thus not significant.The experimental data are reliable, and the models can accurately quantify the process-performance relationship, making them suitable for subsequent process parameter optimization.

Analysis of the second-order regression model for material removal rate shows that the P-values of both linear terms (X_1, X_2, X_3) and quadratic terms (X_1^2, X_2^2, X_3^2) are less than 0.05, indicating significant effects on material removal rate. Based on F-values, the influencing order of the three factors is: polishing pressure > polishing disc speed > polishing liquid flow rate. The significance analysis of the second-order regression model for surface roughness is similar to that for material removal rate. The P-values of its linear terms (X_1, X_2) and quadratic terms (X_1^2, X_2^2, X_3^2) are all below 0.05, exerting significant effects on surface roughness. According to F-values, the influencing order is: polishing pressure > polishing liquid flow rate > polishing disc speed.

ANOVAwas performed to verify the significance of the two response surface prediction models. The ANOVA results of the MRR model are shown in Table 4. The ANOVA results of the surface roughness (Ra) model are shown in Table 5.

Table 4: ANOVA of regression model for MRR

	Sum of squares	df	Mean square	F-value	P-value	significance
model	15649.86	9	1738.87	1411.55	< 0.0001	significant
X_1	8040.39	1	8040.39	6526.88	< 0.0001	significant
X_2	2590.20	1	2590.20	2102.62	< 0.0001	significant
X_3	3888.30	1	3888.30	3156.37	< 0.0001	significant
X_1X_2	4.22	1	4.22	3.43	0.1065	not significant
X_1X_3	4.31	1	4.31	3.50	0.1037	not significant
X_2X_3	0.0121	1	0.0121	0.0098	0.9238	not significant
X_1^2	668.73	1	668.73	542.85	< 0.0001	significant
X_2^2	45.58	1	45.58	37.00	0.0005	significant
X_3^2	317.60	1	317.60	257.81	<0.0001	significant
residuals	8.62	7	1.23			
Lack of fit	5.20	3	1.73	2.02	0.2532	not significant
Pure error	3.43	4	0.8563			
Total deviation	15658.49	16				

Table 5: ANOVA of regression model for Ra

	Sum of squares	df	Mean square	F-value	P-value	significance
model	0.2183	9	0.0243	157.95	< 0.0001	significant
X_1	0.0300	1	0.0300	195.43	< 0.0001	significant
X_2	0.0105	1	0.0105	68.45	< 0.0001	significant
X_3	0.0001	1	0.0001	0.3256	0.5861	not significant
X_1X_2	0.0000	1	0.0000	0.1628	0.6986	not significant
X_1X_3	0.0001	1	0.0001	0.6512	0.4462	not significant
X_2X_3	0.0000	1	0.0000	0.0000	1.0000	not significant
X_1^2	0.1028	1	0.1028	669.37	< 0.0001	significant
X_2^2	0.0521	1	0.0521	339.33	< 0.0001	significant
X_3^2	0.0081	1	0.0081	52.48	0.0002	significant
residuals	0.0011	7	0.0002			
Lack of fit	0.0001	3	0.0000	0.1000	0.9559	not significant
Pure error	0.0010	4	0.0002			
Total deviation	0.2194	16				

Table 6 presents the goodness-of-fit and predictive performance evaluation of the MRR and Ra prediction models. The R^2 values of the two models are 0.9994 and 0.9951, respectively, showing excellent fitting correlation. All statistical indices are qualified, and the superior model performance provides a reliable mathematical basis for multi-objective process optimization.

Table 6: Credibility analysis of prediction models MRR and Ra

number	C.V./%	R^2	Adjusted R^2	Predicted R^2	Adeq precision
Y_1	0.7093	0.9994	0.9987	0.9943	127.8659
Y_2	0.8567	0.9951	0.9888	0.9874	38.6658

Fig.7 shows the comprehensive verification of fitting accuracy and statistical reliability for the response surface models of material removal rate and surface roughness.Figs.7(a) and (b) present the predicted versus measured values of material removal rate and surface roughness, respectively. All data points are closely distributed near the ideal y = x line without obvious systematic deviation, verifying that the regression models can accurately predict polishing performance under various process parameter combinations.Figs.7(c) and (d) display the residual-versus-predicted value plots. The residuals scatter randomly around the zero-residual line with no trend or periodicity, further confirming the absence of systematic errors and the reliability of model fitting.Figs.7(e) and (f) are normal probability plots of residuals. The residual points roughly align with the theoretical normal distribution line without significant deviation, indicating that the residuals follow a normal distribution and meet the basic statistical assumptions of regression analysis. These multi-dimensional verification results consistently demonstrate that the two second-order polynomial regression models established in this study possess excellent prediction accuracy and statistical robustness.

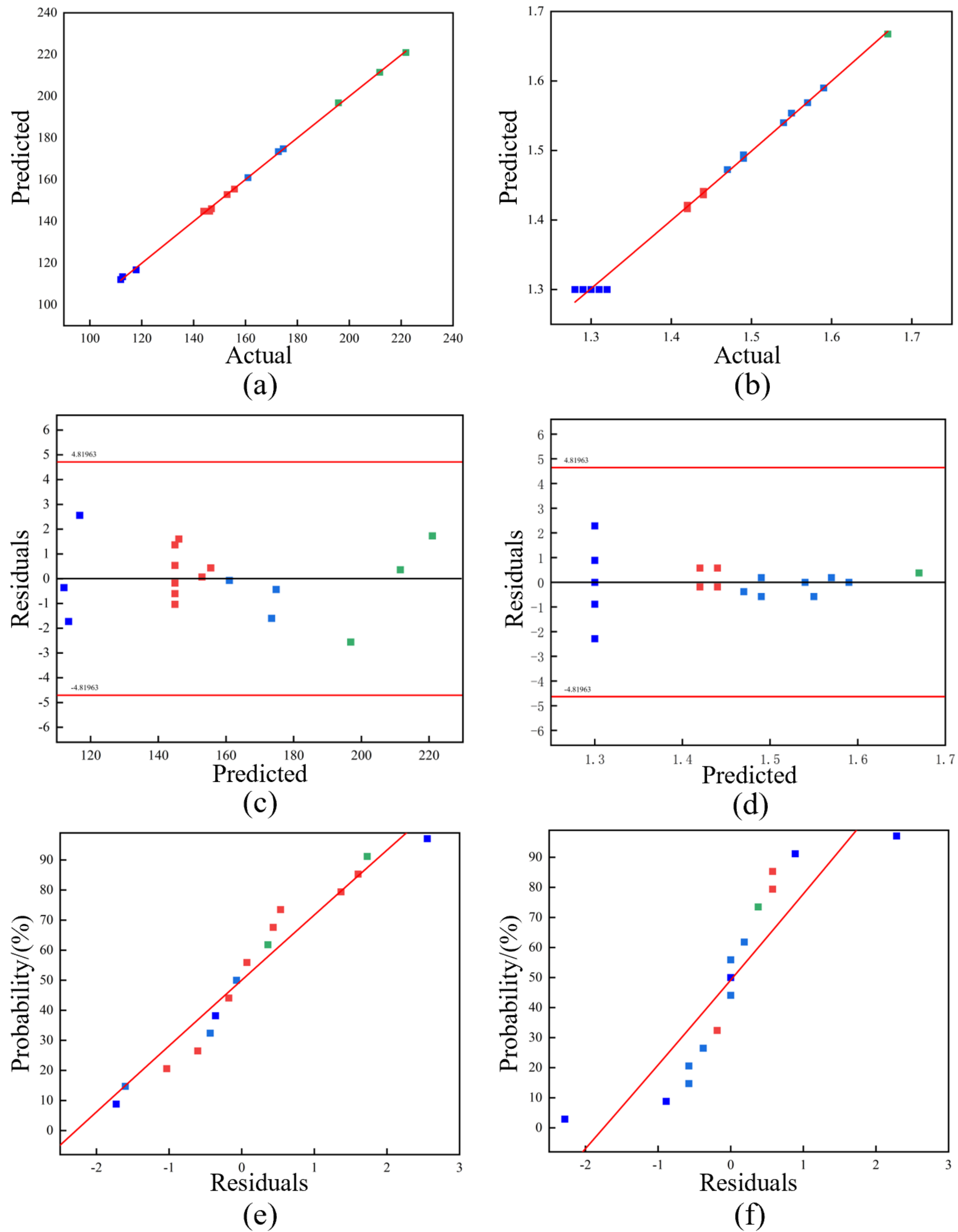

Figure 7: Fitting effect analysis diagrams of MRR and Ra

Fig.8 illustrates the interaction effects of three process parameters on material removal rate. Figs.8(a) and (b) show the interaction between polishing pressure and polishing liquid flow rate: material removal rate increases monotonically with both parameters, and the response surface slope for pressure is steeper, indicating a stronger regulatory effect. The interaction term has $P = 0.1065 > 0.05$, showing no statistically significant synergistic effect.Figs.8(c) and (d) present the interaction between polishing pressure and polishing disc speed: the response surface rises evidently, and material removal rate peaks at the maximum values of both parameters, with

pressure showing a greater influence. The interaction term has $P = 0.1037 > 0.05$, which is not statistically significant.Figs.8(e) and (f) display the interaction between disc speed and flow rate: material removal rate rises slowly with increasing parameters, the response surface is gentle, and the rate fluctuation is far lower than the former two groups. The interaction term has $P = 0.9238 > 0.05$, exerting almost no regulatory effect on the rate.

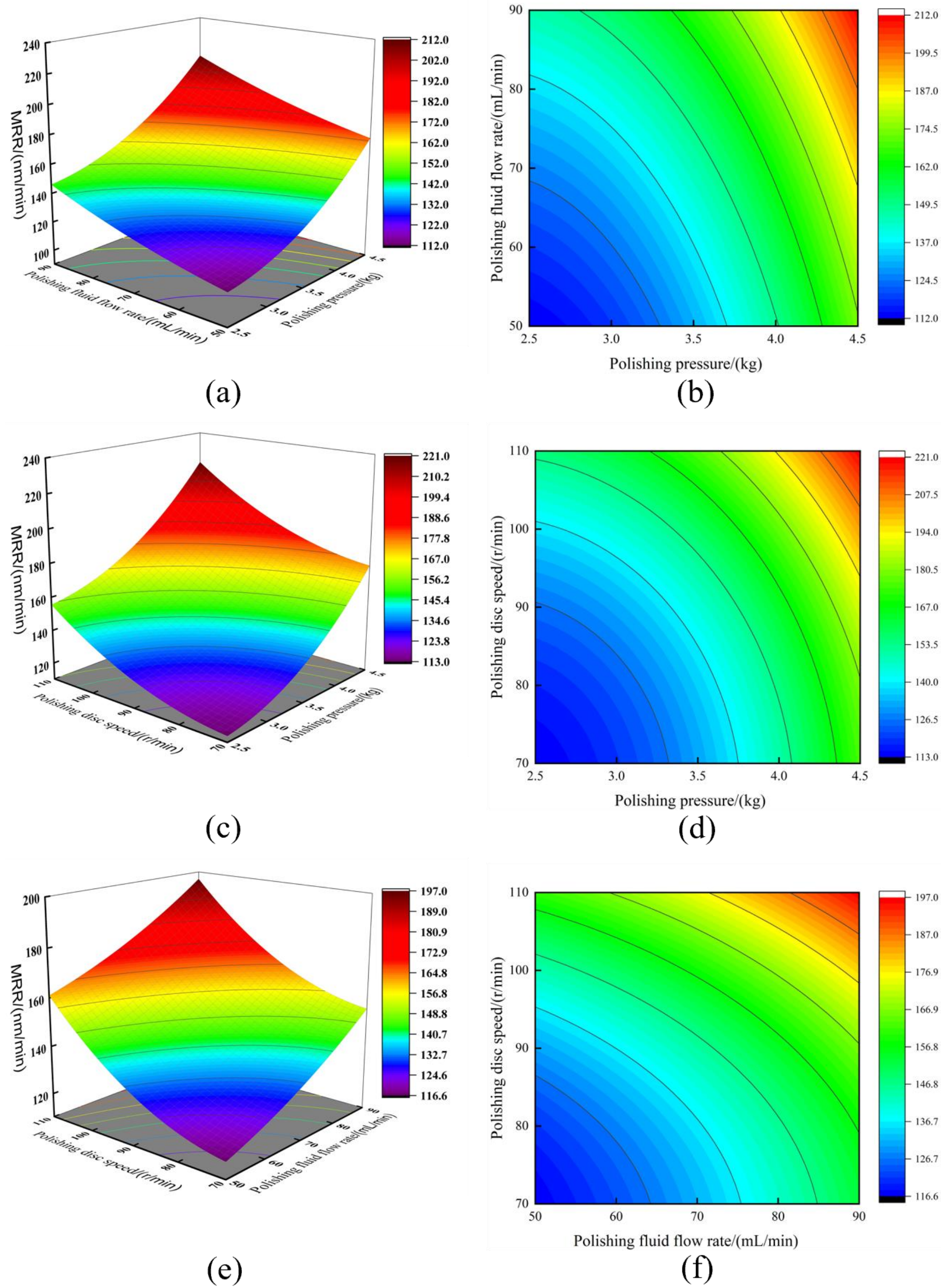

Figure 8: 3D Response Surface and Contour Plots of MRR

Fig.9 shows the interaction effects of three process parameters on the surface roughness of aluminosilicate glass during CMP. Figs. 9(a) and (b) present the interaction between polishing pressure and slurry flow rate: surface roughness shows a parabolic trend of decreasing first and then increasing with the two parameters, reaching the minimum at their medium values. The

response surface of pressure has a larger curvature with a stronger regulatory effect, and their interaction term ($P = 0.6986 > 0.05$) has no statistically significant synergistic effect.Figs.9(c) and (d) show the interaction between polishing pressure and platen rotational speed: the response surface is concave, and roughness drops to the minimum at moderate levels of both parameters and rises rapidly otherwise. Pressure has a greater influence, and the interaction term ($P = 0.4462 > 0.05$) is not statistically significant.Figs. 9(e) and (f) display the interaction between platen rotational speed and slurry flow rate: roughness also decreases first and then increases with the parameters, but the response surface is gentle with much smaller roughness variation than the former two groups. The interaction term ($P = 1.0000 > 0.05$) exerts almost no regulatory effect on roughness.

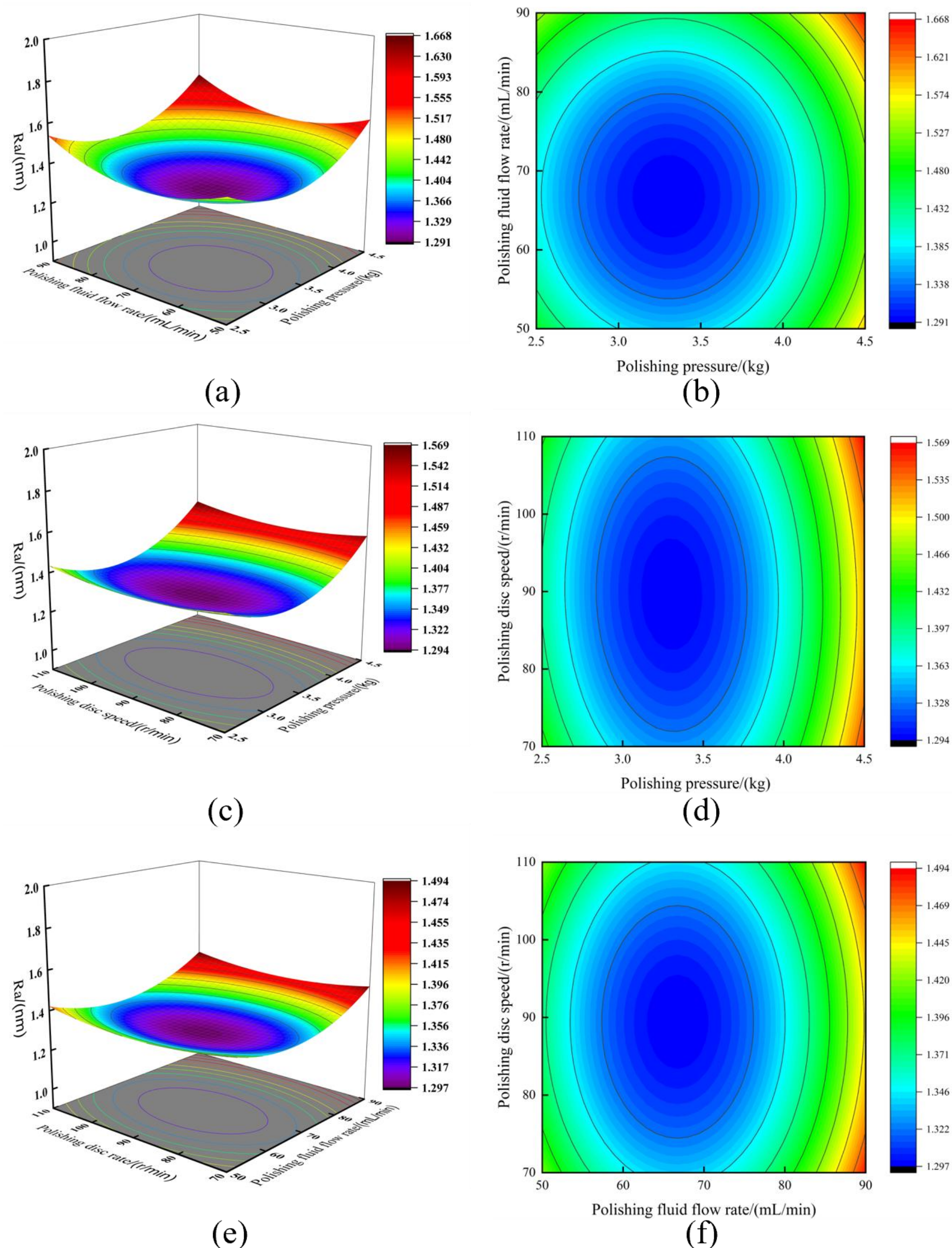

Figure 9: 3D Response Surface and Contour Plots of Ra

Based on the established second-order polynomial prediction models for material removal rate and surface roughness, the CMP process parameters of aluminosilicate glass were optimized. The two response indicators are mutually restrictive. Taking surface roughness as the primary optimization objective, material removal rate was maximized under the constraint of strict processing quality. By setting indicator weights (Table 7), the optimal process parameter combination and corresponding predicted performance were derived (Table 8).

Table 7: Importance of parameters in prediction model

Parameter type	MRR	Ra
Importance level	+++	+++++

Table 8: Optimized CMP parameters and predicted results

Polishing pressure/kg	Polishing liquid flow rate/(mL/min)	Polishing disc speed/(r/min)	MRR/(nm/min)	Ra/(nm)
3.6	71	110	180.153	1.357

Verification experiments of CMP on aluminosilicate glass were conducted using the optimal process parameters from multi-objective optimization, to evaluate the generalization applicability and prediction accuracy of the established response surface model. The performance data are summarized in Table 9, and the 3D surface morphology of the polished glass substrate is shown in Fig.10.The measured material removal rate and surface roughness agree well with the predicted values, with relative errors controlled below 9%, which is reasonable for engineering applications. Surface morphology observations further confirm that the optimal parameters achieve high material removal efficiency while ensuring an ultra-smooth, damage-free surface. The good consistency between experimental and predicted results fully validates the stable and reliable prediction performance of the model, and demonstrates that the optimized parameters are an ideal scheme balancing processing quality and removal efficiency under the experimental conditions.

Table 9: Comparison between predicted and actual values

Target parameter	Predicted value	Actual value	Relative error
MRR/(nm/min)	180.153	196.306	9%
Ra/(nm)	1.357	1.260	7%

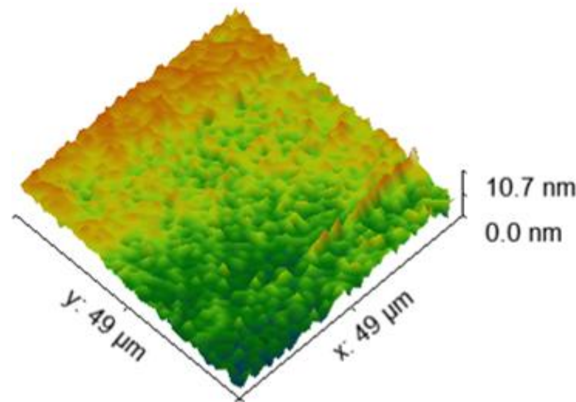

Figure 10: Surface morphology of glass polished with optimized process

4 Conclusion

The CMP process parameters of aluminosilicate glass were systematically optimized via response surface methodology, with the key conclusions as follows:

(1) Single-factor influence law: The material removal rate (MRR) first increases and then decreases with polishing pressure, and rises continuously with increasing flow rate and disc speed. The surface roughness (Ra) decreases first and then increases with the three parameters. Accordingly, the optimal parameter range is determined: pressure 2.5–4.5 kg, flow rate 50–90 mL/min, disc speed 70–110 r/min.

(2) High-precision second-order polynomial prediction models were established (P < 0.0001, R^2 > 0.99). The influence order of process parameters on MRR is: polishing pressure > polishing disc speed > polishing liquid flow rate; while that on Ra is: polishing pressure > polishing liquid flow rate > polishing disc speed. The pairwise interactions among parameters are not significant, and polishing performance is mainly regulated by independent main effects.

(3) Global optimization and verification: Taking the minimization of Ra as the primary constraint, the optimal process combination was determined as: polishing pressure 3.6 kg, polishing liquid flow rate 71 mL/min, polishing disc speed 110 r/min. Experimental verification shows that the measured MRR reaches 196.306 nm/min and Ra is as low as 1.260 nm under these conditions, with the relative error between measured and predicted values below 9%.The optimal balance between processing quality and efficiency is successfully achieved.

References

[1] Nunes B, Pinho I, Cruz Fernandes J, et al. Mechanical properties of ion-exchanged alkali aluminosilicate glass[J]. International Journal of Applied Glass Science, 2022, 14(1): 155-164.

[2] Li M, Dong C, Ma Y, et al. Light-Transmitting Lithium Aluminosilicate Glass-Ceramics with Excellent Mechanical Properties Based on Cluster Model Design[J]. Nanomaterials, 2023, 13(3): 530-542.

[3] Berneschi S, Righini G C, Pelli S. Towards a Glass New World: The Role of Ion-Exchange in Modern Technology[J]. Applied Sciences, 2021, 11(10): 4610-4622.

[4] Krishnan M, Nalaskowski J W, Cook L M. Chemical Mechanical Planarization: Slurry Chemistry, Materials, and Mechanisms[J]. Chemical Reviews, 2010, 110(1): 178-204.

[5] Zantye P B, Kumar A, Sikder A K. Chemical mechanical planarization for microelectronics applications[J]. Materials Science and Engineering: R: Reports, 2004, 45(3): 89-220.

[6] Oh S, Seok J. An integrated material removal model for silicon dioxide layers in chemical mechanical polishing processes[J]. Wear, 2009, 266(7-8): 839-849.

[7] Jianfeng L, Dornfeld D A. Material removal mechanism in chemical mechanical polishing: theory and modeling[J]. IEEE Transactions on Semiconductor Manufacturing, 2001, 14(2): 112-133.

[8] Parthiban P, Das D. Influence of Slurry Flow Rate on Material Removal Rate and

Topography of Chemical Mechanically Planarized c-Plane (0001) GaN Surface[J]. ECS Journal of Solid State Science and Technology, 2017, 6(4): P113-P118.

[9] Mudhivarthi S, Gitis N, Kuiry S, et al. Effects of Slurry Flow Rate and Pad Conditioning Temperature on Dishing, Erosion, and Metal Loss during Copper CMP[J]. Journal of The Electrochemical Society, 2006, 153(5): G372-G386.

[10] Forsberg M. Effect of process parameters on material removal rate in chemical mechanical polishing of Si(100)[J]. Microelectronic Engineering, 2005, 77(3-4): 319-326.

[11] Huang M F, Lin T R, Chiu H C. Effect of machining characteristics on polishing ceramic blocks[J]. The International Journal of Advanced Manufacturing Technology, 2005, 26(9-10): 999-1005.

[12] Wang H, Qin Z, Zhang L, et al. Machine Learning-Driven Optimization of Silicon Carbide Chemical Mechanical Polishing with Surface Roughness Constraints[J]. Langmuir, 2026, 42(3): 2851-2866.

[13] Wang L, Zhou P, Yan Y, et al. Investigation on nanoscale material removal process of BK7 and fused silica glass during chemical-mechanical polishing[J]. International Journal of Applied Glass Science, 2021, 12(2): 198-207.

[14] Deng J, Bai Z, Wen X, et al. Equilibrium between chemical and mechanical parameters for single-crystal SiC in Electro-Fenton chemical-mechanical polishing[J]. Diamond and Related Materials, 2025, 152: 111979- 111986.

[15] Irfan H M, Lee C Y, Mazumdar D, et al. Improvement of Material Removal Rate and Within Wafer Non-Uniformity in Chemical Mechanical Polishing Using Computational Fluid Dynamic Modeling[J]. Journal of Manufacturing and Materials Processing, 2025, 9(3): 95-107.